A New Fault-Tolerant Strategy Based on a Modified Selective Harmonic Technique for Three-Phase Multilevel Converters With a Single Faulty Cell

Mohsen Aleenejad, Hamid Mahmoudi, Parvin Moamaei, and Reza Ahmadi, *Member, IEEE*

***Abstract*—This paper proposes a new fault-tolerant strategy to revamp performance of three-phase multilevel converters with a single faulty switch. The proposed fault-tolerant strategy is based on the application of a modified selective harmonic elimination (SHE) technique in conjunction with the fundamental phase-shift compensation method. The proposed fault-tolerant strategy makes the most use of the converter capacity in the faulty condition, generates balanced line voltages, and eliminates a wide range of lower order harmonics to limit the total harmonic distribution of the converter voltages in the faulty condition. In this paper, first, a brief background about cascaded H-bridge multilevel converters and SHE technique is provided. Then, the proposed fault-tolerant strategy and the modified SHE technique are presented. Finally, several experimental results are provided to validate the operation of the proposed strategy.**

***Index Terms*—Fault-tolerant strategy, fundamental phase-shift compensation (FPSC), multilevel converter, selective harmonic elimination (SHE).**

I. Introduction

RECENTLY, the use of multilevel converters has been increasing rapidly in industrial applications for medium- to high-power conversion ratings. Compared with conventional inverters, they offer enhanced characteristics such as higher efficiency, lower total harmonic distortion (THD), and lower switching voltage stress [1]–[3], at the price of an increased number of power electronic switches. In a converter topology, as the number of power electronic devices increases, the possibility of fault occurrence increases, and accordingly the converter's reliability decreases [4]–[6]. Due to the extreme monetary ramifications of the interruption in the operation apparatus, it is critical for the power converters utilized in commercial and industrial to be highly reliable. Consequently, developing fault-tolerant operation techniques for multilevel converters has always been an area of interest for researchers [7]–[10].

In recent years, several fault-tolerant operation methods for multilevel converters have been proposed in the literature. All of the proposed methods can be classified into two categories: strategies that reconfigure the converter hardware structure in case of a fault occurrence, and strategies that modify the converter control technique and modulation method in case of a fault occurrence [11]–[14]. A few fault-tolerant methods use a combination of hardware-based reconfiguration and control-based revision methods as well. The fault-tolerant strategies proposed in [15]–[17] are examples of employing additional power electronic devices and reconfiguring the converter topology after fault occurrence. Because of their modular structure and redundant cells, the cascaded H-bridge (CHB) converters are one of the well suited options for hardware-based techniques [18], [19]. The fault-tolerant methods presented in [20]–[25] are some of the proposed strategies that change the control algorithm and revise the modulation technique after fault diagnosis. In [23] and [24], some fault-tolerant techniques based on carrier-based pulse width modulation (CB-PWM) method are presented. In the event of a fault, the faulty phase generates lower voltage compared with the healthy phase. In these fault-tolerant methods, the phase shifts between the healthy and faulty voltages are modified to produce balanced line-to-line voltages. In [25], a work based on fundamental phase shift compensation PWM is presented. In this paper, the angles of the converter phase voltages are revised through changing the phase shifts of the reference signals. This leads to balanced line-to-line voltages; although the third-order harmonics cannot be eliminated naturally, and thus, the THD of the line-to-line voltages is increased in the faulty condition. Some of the mentioned fault-tolerant strategies have found their way into commercial applications as well [26]. For example, a family of medium-voltage cell-based inverters which are called the "Siemens ROBICON Perfect Harmony" drives [27], utilizes the redundancy of the power cells together with the neutral shift control [22] for the post fault operation.

The purpose of this paper is to propose a new fault-tolerant strategy for control of a multilevel converter with a single faulty switch. The proposed fault-tolerant strategy generates balanced line-to-line voltages without bypassing any unnecessary converter elements, makes better use of the converter capacity and generates higher output voltages, makes the third-order harmonics of the phase voltages cancel out naturally, and eliminates a wide range of low-order harmonics of the voltages to limit the THDs in the event of a fault. The proposed strategy exploits the advantages of the selective harmonic elimination (SHE) methods in conjunction with the FPSC technique to generate balanced voltages and manipulate voltage harmonics at the same time. However, due to the distinctive requirement of the strategy to manipulate both the amplitude and angle of the harmonics,

Manuscript received December 15, 2014; revised April 6, 2015; accepted May 31, 2015. Date of publication June 11, 2015; date of current version November 30, 2015. Recommended for publication by Associate Editor J. R. Rodriguez.

The authors are with the Department of Electrical and Computer Engineering, Southern Illinois University, Carbondale, IL 62901 USA (e-mail: mohsen@siu.edu; hamid@siu.edu; parvin@siu.edu; ahmadi@siu.edu).

Color versions of one or more of the figures in this paper are available online at http://ieeexplore.ieee.org.

Digital Object Identifier 10.1109/TPEL.2015.2444661

the conventional SHE techniques are not a suitable basis for the proposed strategy. Therefore, in this paper, a modified SHE technique that can be used as the basis for the proposed strategy is developed. Although the proposed strategy is applicable to several classes of multilevel converters with three or more voltage levels, in this paper, the operation of a seven-level CHB multilevel converter with a single faulty switch is revamped by the proposed fault-tolerant strategy as a case study.

The structure of the paper is as follows: in Section II, a concise review of CHB converters' construction and operation is provided. In Section III, the principles of conventional SHE techniques are reviewed and the reasoning for requiring a modified SHE technique is presented. The basic Fourier formulations for the SHE problem are also provided in this section. Section IV introduces the proposed fault-tolerant strategy and the developed modified SHE technique. Section V describes the application of the proposed strategy to a prototype seven-level CHB converter and provides several experimental waveforms that verify the capabilities and merits of the proposed strategy. Section VI concludes this paper.

II. CHB Multilevel Converter

The CHB multilevel converters are commonly used in industrial applications on account of their inherent superior properties such as modular structure, simple physical layout, and offering of more redundant switching states than other multilevel topologies. Fig. 1(a) in [28] illustrates the circuit topology of a seven-level CHB converter. The proposed fault-tolerant strategy in this paper is presented by describing its application to the converter of this figure. As pictured, each phase of this converter is made up of three H-bridge cells. Fig. 1(b) in [28] displays an H-Bridge cell assembled from four IGBT switches S_1–S_4. Labeling the input terminal voltage of an H-bridge as V_{dc}, the output terminal voltage can be made equal to V_{dc}, 0, or $-V_{dc}$ by properly firing the switches [29]. Therefore, due to the series connection of three H-bridge cells in each phase of the CHB converter of Fig. 1(a) in [28], seven voltage levels can be generated by each phase of this converter: $-3V_{dc}$, $-2V_{dc}$, V_{dc}, 0, V_{dc}, $2V_{dc}$, and $3V_{dc}$ [30].

III. Selective Harmonic Elimination

The SHE modulation technique can be utilized to make a multilevel inverter to generate ac voltages with favorable harmonic properties. Exploiting this method leads to obtaining a certain arrangement of switching angles for each phase of the converter. The calculated switching angles mark the switching transition instances for each phase. At each transition instance, the generated phase voltage level is transitioned to another level by altering the status of conduction of the switches. The SHE method uses the Fourier analysis of the voltages of the converter to calculate the aforementioned switching angles. For each modulation index, the Fourier coefficient of the fundamental harmonic of the output voltage is set to the desired value, while coefficients for undesired low-order harmonics are set to zero. This yields a system of nonlinear equations that needs to be solved numerically for switching angles. The calculated switching angles for each modulation index are stored in a look-up table on a programmable memory in a digital controller. The controller fetches the switching angles from the memory according to the current modulation index and generates the switching signals based on the switching angles and a specific voltage level transition arrangement [31]–[33].

The voltage level transition arrangement identifies the voltage level to be generated at each transition instance. Different transition arrangements are proposed and studied in the literature [34]–[37]. One important property of different transition arrangements is the number of switching transitions allocated in each period of the switching function. A high number of switching transitions provide more flexibility for manipulation of the harmonic properties of the generated voltages, although it also nullifies the low-frequency switching advantage that comes inherently with SHE-PWM, resulting in increased switching power losses. Furthermore, it leads to a large-scale system of equations that needs to be solved for finding the switching angles, resulting in increased calculation complexity [38]–[41].

As mentioned, in order to reduce the computation complexity and the converter's switching frequency, it is desirable to decrease the number of the switching angles. In this paper, only 14 switching angles are allocated for each half period of the phase voltage. Decreasing the number of switching angles leads to less flexibility for manipulation of the harmonic components of the waveforms [35], [36]. Consequently, to increase the degree of freedom, in this paper, a half-wave symmetry is considered for the switching functions. By employing the half-wave symmetric SHE-PWM, not only the amplitude of each individual harmonic but also the phase angle of the harmonics can be manipulated.

A general seven-level voltage waveform with half-wave symmetry and 14 switching angles (φ_1 to φ_{14}) is illustrated in Fig. 1(a). As pictured, the envisioned voltage level transitions include two transitions between 0 and $+V_{dc}$, two transitions between $+V_{dc}$ and $+2V_{dc}$, and ten transitions between $+2V_{dc}$ and $+3V_{dc}$. The corresponding Fourier coefficients for the seven-level voltage waveform of Fig. 1(a) can be found from equation (1) as shown at the bottom of the next page where V_{abcn} represents the phase voltages, A_{abcn} and B_{abcn} are the Fourier coefficients of the phase voltages, w is the angular frequency, n is the order of harmonic, i is ith switching angle, and a_n and b_n are the sign coefficients, [35] and [36].

In case of a single faulty switch (the focus of this paper) in the CHB converter, based on the location of the faulty switch and the fault type, the faulty phase of the converter fails to generate one of the seven feasible voltage levels. The six-level voltage waveform generated by the faulty phase is asymmetric around zero, thus containing undesirable dc-offset component. As a result, after fault diagnosis, typically the faulty H-bridge cell is bypassed altogether to make the voltage waveform symmetric around zero and prevent generation of the dc-offset voltage. This reduces the achievable voltage levels by the faulty phase to only five levels: $-2V_{dc}, V_{dc}, 0, V_{dc}, 2V_{dc}$. A general five-level voltage waveform with half-wave symmetry and 14 switching angles is illustrated in Fig. 1(b). The voltage level transitions include two transitions between 0 and $+V_{dc}$, and 12 transitions between

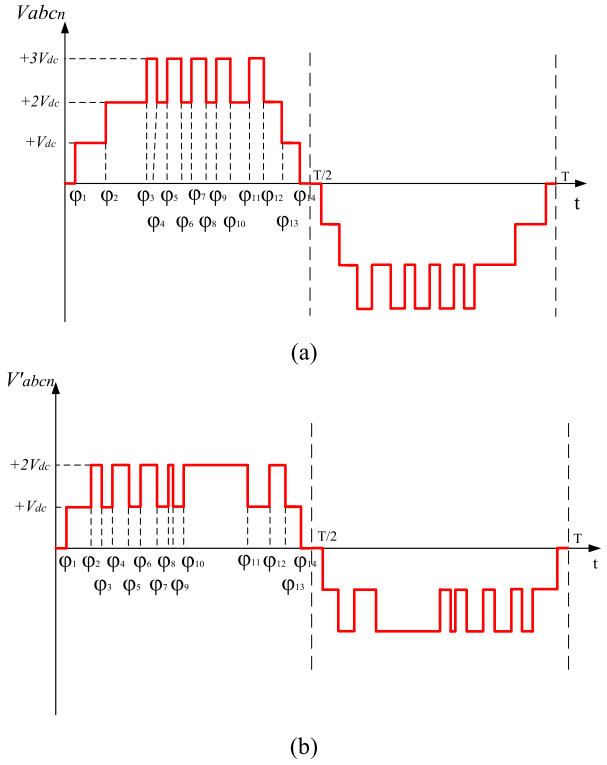

Fig. 1. (a) General seven-level voltage waveform realizable by a CHB converter. (b) Five-level voltage waveform achievable by a CHB converter with one bypassed H-bridge cell.

$+V_{\rm dc}$ and $+2V_{\rm dc}$. The corresponding Fourier coefficients for the five-level voltage waveform of Fig. 1(b) can be found from equation (2) as shown at the bottom of the page, [35] and [36].

Note that the five-level inverter quantities in (2) are differentiated from the seven-level inverter quantities in (1) by prime symbols (V'_{abcn}, A'_{abcn}, and B'_{abcn}).

IV. Proposed Fault-Tolerant Strategy

As mentioned previously, in case of a single faulty switch in the CHB converter, the achievable voltage levels by the faulty phase are reduced to five levels. In this situation, the healthy phases generate seven voltage levels, while the faulty phase generates five voltage levels. Consequently, the amplitude of the voltages generated by the healthy phases is equal to 3 $V_{\rm dc}$ (referred to as 3 p.u. hereinafter), while the amplitude of the voltage generated by the faulty phase is reduced to 2 $V_{\rm dc}$ (referred to as 2 p.u. hereinafter). This leads to the generation of unbalanced line-to-line voltages. The phasor diagram of Fig. 2(a) elaborates on the operation of the converter in this condition. According to this figure, the amplitude of $V_{\rm bc}$ is equal to 5.19 p.u., while the amplitudes of $V_{\rm ab}$ and V_{ca} are equal to 4.35 p.u.

The conventional solution to the problem of unbalanced line-to-line voltages is to bypass two additional H-bridge cells in the healthy phases of the converter, thus reducing the reachable voltage levels by all phases to five levels. This results in balanced operation; however, it renders three H-bridge cells non-operational, resulting in a significant reduction in the maximum achievable converter voltage. The phasor diagram of Fig. 2(b) illustrates the converter voltages in this condition. According to this figure, the amplitude of the line-to-line voltages is reduced from 5.19 p.u. (for a healthy converter) to 3.46 p.u.

The proposed fault-tolerant strategy does not bypass any additional H-bridge cells; instead, it adopts the FPSC technique to modify the angles of the fundamental harmonics of the phase voltages (see $\theta_{ab}, \theta_{bc}, \theta_{ca}$ in Fig. 2) to generate line-to-line voltages with balanced fundamental harmonics. The conventional FPSC technique discussed in [25] utilizes the CB-PWM modulation to modify the phase voltage angles; however, the proposed method adopts FPSC to modify merely the angles of the fundamental harmonics of the phase voltages. Fig. 2(c) demonstrates how modifying the fundamental phase angles can lead to balanced fundamental line-to-line voltages. According to this

$$\begin{cases} V_{abcn} = \sum_{n=1}^{\infty} \frac{1}{n} \frac{2V_{\rm dc}}{\pi} \left(A_{abcn} \times \cos\left(nwt\right) + B_{abcn} \times \sin\left(nwt\right)\right) \\ A_{abcn} = \sum_{i=1}^{14} a_n \sin(n\varphi_i) \quad \begin{cases} a_n = -1 & \text{for } \; i = 4,6,8,10,12,13,14 \\ a_n = 1 & \text{for } \; i = 1,2,3,5,7,9,11 \end{cases} \\ B_{abcn} = \sum_{i=1}^{14} b_n \cos(n\varphi_i) \quad \begin{cases} b_n = -1 & \text{for } \; i = 4,6,8,10,12,13,14 \\ b_n = 1 & \text{for } \; i = 1,2,3,5,7,9,11 \end{cases} \end{cases} \tag{1}$$

$$\begin{cases} V'_{abcn} = \sum_{n=1}^{\infty} \frac{1}{n} \frac{2V_{\rm dc}}{\pi} \left(A'_{abcn} \times \cos(nwt) + B'_{abcn} \times \sin(nwt)\right) \\ A'_{abcn} = \sum_{i=1}^{14} a_n \sin(n\varphi_i) \quad \begin{cases} a_n = -1 & \text{for } i = 3,5,7,9,11,13,14 \\ a_n = 1 & \text{for } i = 1,2,4,6,8,10,12 \end{cases} \\ B'_{abcn} = \sum_{i=1}^{14} b_n \cos(n\varphi_i) \quad \begin{cases} b_n = -1 & \text{for } i = 3,5,7,9,11,13,14 \\ b_n = 1 & \text{for } i = 1,2,4,6,8,10,12 \end{cases} \end{cases} . \tag{2}$$

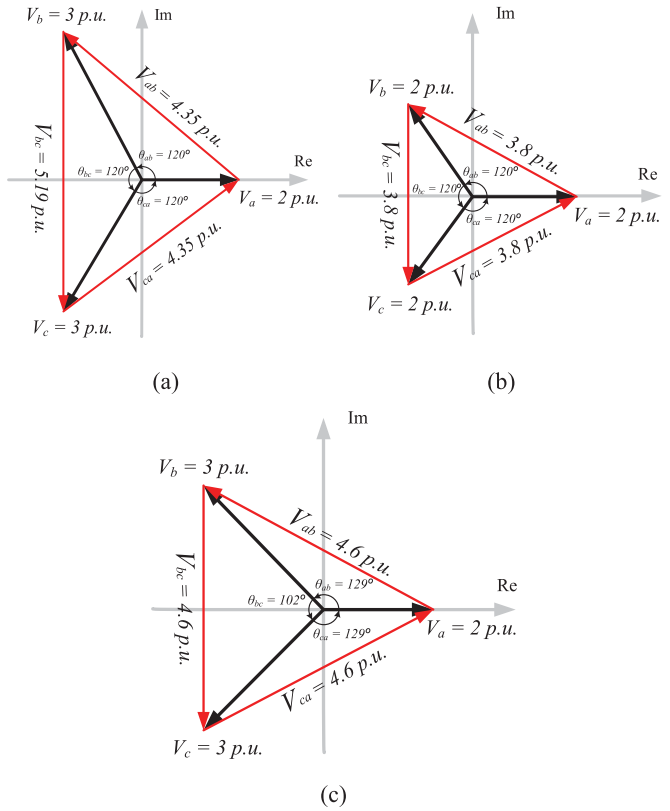

Fig. 2. Phasor diagram of fundamental harmonics of phase voltages in a CHB converter under faulty condition. (a) Faulty cell is bypassed and the line-to-line voltages are unbalanced. (b) Two additional cells are bypassed, resulting in balanced operation with reduced voltage amplitude. (c) Phase angles are modified according to the proposed method to generate balanced line-to-line voltages with less voltage reduction.

figure, although the amplitude of the fundamental harmonics of phase voltages (V_a, V_b, V_c) are not equal, by properly adjusting the fundamental phase angles($\theta_{ab}, \theta_{bc}, \theta_{ca}$), the amplitude of the fundamental line-to-line voltages (V_{ab}, V_{bc}, V_{ca}) are made all equal (4.6 p.u.). The FPSC strategy makes better use of the converter capacity by keeping all the H-bridge cells except the faulty one operational. This results in improved converter performance and higher line-to-line voltage amplitude in comparison to conventional methods. Comparing Fig. 2(b) and (c), the amplitude of the fundamental line-to-line voltages generated using the modified FPSC strategy (4.6 p.u.) is significantly higher than the voltages generated using the conventional methods (3.46 p.u.).

The fundamental phase angles that result in balanced fundamental line-to-line voltages can be found by solving the following set of equations for θ_{ab}, θ_{bc}, and θ_{ca} [22]

$$\begin{cases} V_a^2 + V_b^2 - 2V_aV_b\cos(\theta_{ab}) = V_b^2 + V_c^2 - 2V_bV_c\cos(\theta_{bc}), \\ V_b^2 + V_c^2 - 2V_bV_c\cos(\theta_{bc}) = V_c^2 + V_a^2 - 2V_cV_a\cos(\theta_{ca}), \\ \theta_{ab} + \theta_{bc} + \theta_{ca} = 360^o \end{cases} \tag{3}$$

where θ_{ab}, θ_{bc}, and θ_{ca} are the phase shifts between fundamental harmonics of the phase voltages, and V_a, V_b, and V_c are the amplitude of the fundamental harmonics of three-phase voltages. As mentioned previously, each healthy phase of a seven-level CHB converter can generate a maximum voltage of 3 p.u., while the faulty phase can generate a maximum voltage of only 2 p.u. However, in practice, it is possible to control the faulty phase in the overmodulation region and generate up to 2.2-p.u. voltage. Assuming phase "a" is the faulty phase, as an example, and thus setting $V_a = 2.2$ p.u. and $V_b = V_C = 3$ p.u. in (3) yields $\theta_{ab} = \theta_{ca} = 131°$ and $\theta_{ba} = 98°$. Therefore, for generating balanced fundamental line-to-line voltages, the phase shifts between the fundamental harmonics of the three-phase voltages should be adjusted according to the obtained values (goal 1). However, to ensure that the third-order harmonics in the phase voltages will cancel out naturally in the line-to-line voltages, their amplitudes should be made equal and the phase shifts between them should be made equal to zero degrees (goal 2). Additionally, the amplitude of the remaining undesirable lower order harmonics should be zeroed (goal 3).

The SHE method can be utilized in conjunction with the modified FPSC technique to reach the three aforementioned goals in order to get a set of balanced line-to-line voltages, eliminate third-order harmonics naturally, and eliminate a range of low-order harmonics. The conventional SHE strategy only manipulates the amplitude of the harmonics by deriving a specific switching function for one of the three phases of the converter [33], [34], [42]. The other two phases use the same derived switching function with $\pm 120°$ phase shifts. However, in this paper, both the amplitude and angle of the harmonics need to be manipulated. Furthermore, because of the unequal phase shifts between the fundamental harmonics of the three-phase voltages, the switching functions for the three phases are no longer similar with only a ± 120 phase shift. Rather, each phase requires a unique switching function. Therefore, the problem of finding switching angles should be solved for the three phases simultaneously and a unique result should be found for each individual phase. A modified SHE strategy capable of manipulating both the amplitude and angle of harmonics, and generating unique switching functions for each phase of the converter is proposed in the remainder of this section.

As mentioned, the first goal is to set the amplitude of the fundamental harmonics of the three-phase voltages equal to some desired values while making the phase shifts between them equal to the calculated angles θ_{ab}, θ_{bc}, and θ_{ca}. Based on (1) and (2), and assuming a fault on phase "a", the following system of equations can be assembled to adjust the amplitude and angle of the fundamental harmonics according to the requirements of the first goal

$$\begin{cases} \dfrac{M'\pi}{2} = \sqrt{A_{a1}'^2 + B_{a1}'^2} \\ \dfrac{M\pi}{2} = \sqrt{A_{b1}^2 + B_{b1}^2} = \sqrt{A_{c1}^2 + B_{c1}^2} \\ \operatorname{arctg}\left(\dfrac{B_{b1}}{A_{b1}}\right) - \operatorname{arctg}\left(\dfrac{B'_{a1}}{A'_{a1}}\right) = \theta_{ab} \\ \operatorname{arctg}\left(\dfrac{B_{c1}}{A_{c1}}\right) - \operatorname{arctg}\left(\dfrac{B'_{a1}}{A'_{a1}}\right) = -\theta_{ca} \end{cases} \tag{4}$$

where M is the modulation index for the two healthy phases ("b" and "c") and M' is the modulation index for the faulty phase ("a").

The next goal is to manipulate the amplitude and phase of the third-order harmonics. As mentioned, the amplitude of the third-order harmonics need to be made equal, while the phase shifts between them need to be set to 0°. This can be done by solving (4) in conjunction with the following equation:

$$\begin{cases} \sqrt{A_{a3}'^2 + B_{a3}'^2} = \sqrt{A_{b3}^2 + B_{b3}^2} = \sqrt{A_{c3}^2 + B_{c3}^2} \\ \operatorname{arctg}\left(\dfrac{B_{b3}}{A_{b3}}\right) - \operatorname{arctg}\left(\dfrac{B'_{a3}}{A'_{a3}}\right) = 0 \\ \operatorname{arctg}\left(\dfrac{B_{c3}}{A_{c3}}\right) - \operatorname{arctg}\left(\dfrac{B'_{a3}}{A'_{a3}}\right) = 0 \end{cases} . \quad (5)$$

The third goal is to eliminate as much low-order harmonics as possible. The low-order harmonics up to the 13th order can be eliminated by solving (4) and (5) in conjunction with the following equation:

$$\sqrt{A_{an}'^2 + B_{an}'^2} = \sqrt{A_{bn}^2 + B_{bn}^2} = \sqrt{A_{cn}^2 + B_{cn}^2} = 0 \quad (6)$$

for $n = 5, 7, 9, 11, 13$. As a result, to reach the three aforementioned goals at the same time, (4)–(6) should be solved simultaneously for the switching angles.

As mentioned previously, the set of switching angles for each phase is unique; therefore, the switching angles for phase "a" are denoted as (α_1 to α_{14}), phase "b" as (β_1 to β_{14}), and phase "c" as (γ_1 to γ_{14}) hereinafter. Equations in (4)–(6) need to be solved according to some limiting constraints on the switching angles

$$0^\circ < \alpha_k < \alpha_{k+1} < 180^\circ \quad k = 1, 2, 3, \ldots, 13 \quad (7)$$

$$\beta_0 < \beta_k < \beta_{k+1} < (\beta_0 + 180^\circ) \quad k = 1, 2, 3, \ldots, 13 \quad (8)$$

$$\gamma_0 < \gamma_k < \gamma_{k+1} < (\gamma_0 + 180^\circ) \quad k = 1, 2, 3, \ldots, 13. \quad (9)$$

The inequality in (7) rationalizes that the 14 switching angles for phase "a" are to be distributed consecutively in a half period of the switching function starting from 0 °. Inequalities in (8) and (9) convey the same idea except that the starting points for phases "b" and "c" (β_0 and γ_0) are unknown and thus need to be found while solving (4)–(6). Nevertheless, since the angles of fundamental harmonics of phases "b" and "c" are being set, respectively, θ_{ab} and θ_{bc} degrees apart from that of phase "a," it is expected that the values of β_0 and γ_0 be found close to θ_{ab} and $-\theta_{ca}$ degrees.

Although it is possible to solve (4)–(6) according to the constraints in (7)–(9), the problem of unknown range of switching angles for phase "b" and "c" increases the required computational effort significantly. To alleviate this problem and reduce the overall complexity, an innovative way of reformulating (4)–(6) is devised. To reformulate the problem, the three switching functions for the three phases are defined in the range of 0° to 180°, and the fundamental harmonics are placed at the same angle for solving. This is equivalent to making the following modifications to the original formulation:

$$\begin{cases} \operatorname{arctg}\left(\dfrac{B_{b1}}{A_{b1}}\right) - \operatorname{arctg}\left(\dfrac{B'_{a1}}{A'_{a1}}\right) = 0 \\ \operatorname{arctg}\left(\dfrac{B_{c1}}{A_{c1}}\right) - \operatorname{arctg}\left(\dfrac{B'_{a1}}{A'_{a1}}\right) = 0 \\ \begin{cases} 0 < \alpha_k < \alpha_{k+1} < 180 \\ 0 < \beta_k < \beta_{k+1} < 180 \\ 0 < \gamma_k < \gamma_{k+1} < 180 \end{cases} \quad k = 1, 2, 3, ..., 13. \end{cases} \quad (10)$$

The obtained switching functions are then shifted for θ_{ab} and $-\theta_{ca}$ degrees, respectively, to shift the fundamental harmonics to the desired angles (θ_{ab} and $-\theta_{ca}$). However, to maintain the phase shift between the third-order harmonics at 0 ° after shifting the switching functions, (4)–(6) need to be further modified prior to solving. Subsequent to shifting the obtained switching functions for θ_{ab} and$-\theta_{ca}$ degrees, the third-order harmonics of phase "b" and "c" will be placed at $3 \times \theta_{ab}$ and $-3 \times \theta_{ca}$ degrees, respectively, [28], [43]. However, it is desirable that these harmonics be placed at $\pm 360^\circ$ after shifting. As a result, it is possible to adjust the angle of these harmonics prior to shifting, such that after shifting, the angles end up at$\pm 360^\circ$. Adjusting the angles prior to shifting can be carried out according to the following general formula for the third-order harmonic of a waveform

$$\theta_{\text{new}} = \theta_{\text{old}} \pm 3 \times \theta_{\text{shift}} \quad (11)$$

where θ_{shift} is the amount of shift of the waveform, θ_{old} is the angle of the third harmonic of the waveform before shifting, and θ_{new} is the angle of the third harmonic of the waveform after shifting. According to (11), the angle of the third harmonic of phase "b" should be set to $\theta_{\text{old}} = 360 - 3 \times \theta_{ab}$ prior to shifting. Similarly, the angle of the third harmonic of phase "c" should be set to $\theta_{\text{old}} = -360 + 3 \times \theta_{ca}$ prior to shifting. This is equivalent to making the following modifications to the original formulation:

$$\begin{cases} \operatorname{arctg}\left(\dfrac{B_{b3}}{A_{b3}}\right) - \operatorname{arctg}\left(\dfrac{B'_{a3}}{A'_{a3}}\right) = 360 - 3 \times \theta_{ab} \\ \operatorname{arctg}\left(\dfrac{B_{c3}}{A_{c3}}\right) - \operatorname{arctg}\left(\dfrac{B'_{a3}}{A'_{a3}}\right) = -360 + 3 \times \theta_{ca} \end{cases} \quad (12)$$

considering the modifications reflected in (10) and (12), the final system of equations that needs to be solved to reach all three

aforementioned goals is

$$\begin{cases} \dfrac{M'\pi}{2} = \sqrt{A_{a1}'^2 + B_{a1}'^2} \\ \dfrac{M\pi}{2} = \sqrt{A_{b1}^2 + B_{b1}^2} = \sqrt{A_{c1}^2 + B_{c1}^2} \\ \operatorname{arctg}\left(\dfrac{B_{b1}}{A_{b1}}\right) - \operatorname{arctg}\left(\dfrac{B'_{a1}}{A'_{a1}}\right) = 0 \\ \operatorname{arctg}\left(\dfrac{B_{c1}}{A_{c1}}\right) - \operatorname{arctg}\left(\dfrac{B'_{a1}}{A'_{a1}}\right) = 0 \\ \sqrt{A_{a3}'^2 + B_{a3}'^2} = \sqrt{A_{b3}^2 + B_{b3}^2} = \sqrt{A_{c3}^2 + B_{c3}^2} \\ \operatorname{arctg}\left(\dfrac{B_{b3}}{A_{b3}}\right) - \operatorname{arctg}\left(\dfrac{B'_{a3}}{A'_{a3}}\right) = 360 - 3 \times \theta_{ab} \\ \operatorname{arctg}\left(\dfrac{B_{c3}}{A_{c3}}\right) - \operatorname{arctg}\left(\dfrac{B'_{a3}}{A'_{a3}}\right) = -360 + 3 \times \theta_{ca} \\ \sqrt{A_{an}'^2 + B_{an}'^2} = \sqrt{A_{bn}^2 + B_{bn}^2} = \sqrt{A_{cn}^2 + B_{cn}^2} = 0, \\ \qquad n = 5, 7, 9, 11, 13 \end{cases} \tag{13}$$

According to

$$\begin{cases} 0 < \alpha_k < \alpha_{k+1} < 180 \\ 0 < \beta_k < \beta_{k+1} < 180 \\ 0 < \gamma_k < \gamma_{k+1} < 180 \end{cases} \quad k = 1, 2, 3, \ldots, 13\,.$$

The calculated switching angles (α_1 to α_{14}) belong to the faulty phase (phase "a" in this paper), (β_1 to β_{14}) belong to the phase with positive-voltage sequence relative to the faulty phase (phase "b" in this paper), and (γ_1 to γ_{14}) belong to the phase with negative-voltage sequence (phase "c" in this paper). Similar to conventional SHE, the switching angles are calculated for a range of modulation indexes using (13) prior to converter operation and are stored in a look-up table on the converter's digital controller. In a practical application, in case of a single fault, the converter controller stops using the normal SHE look-up table and uses the look-up table generated using (13) for fault-tolerant operation. Although a seven-level inverter is employed in this paper for the demonstration of the proposed fault tolerant strategy, this method can easily be expanded to multilevel inverters with higher (or lower) number of voltage levels. A flowchart of operation of a multilevel inverter with the proposed fault-tolerant strategy is depicted in Fig. 3.

V. Experimental Results

In this section, the proposed fault-tolerant strategy will be utilized to revamp the performance of a prototype seven-level CHB converter with a faulty switch in phase "a". As mentioned previously, in case of a single faulty H-bridge cell in phase "a", based on (3), the phase shift between the fundamental harmonic of the inverter phase voltages needs to be adjusted to $\theta_{ab} = \theta_{ca} = 131^\circ$. Additionally, to generate the highest possible voltage in the faulty phase, M' should be set to 2.2, while M is varied from 2.2 to 3. Using the modified fundamental phase angles and the value of M', it is possible to solve (13) for a range

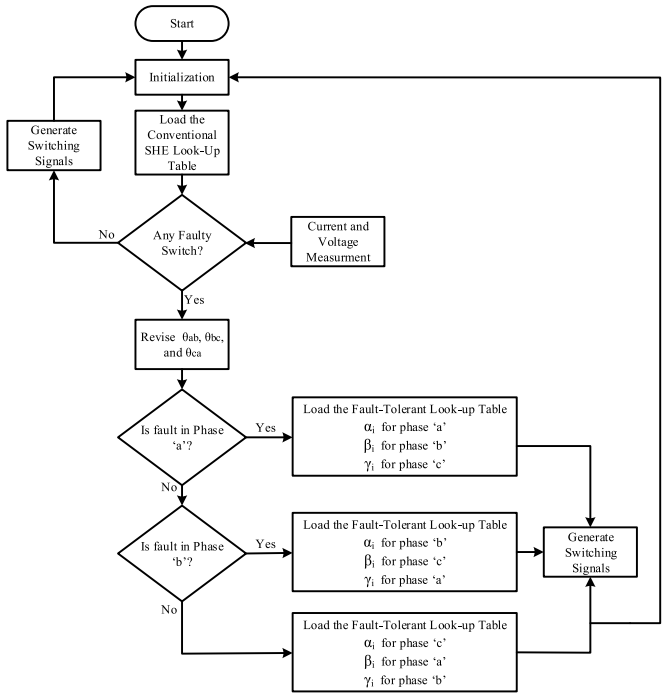

Fig. 3. Flowchart of the operation of a multilevel converter with the proposed fault-tolerant strategy.

TABLE I
Switching Angles for Phase "a"

α_1	α_2	α_3	α_4	α_5	α_6	α_7
8.47	9.28	9.86	25.25	32.10	35.19	89.76
α_8	α_9	α_{10}	α_{11}	α_{12}	α_{13}	α_{14}
90.23	144.80	147.89	154.74	170.13	170.71	171.52

of M (2.2 to 3). A possible set of solutions for the switching angles are shown in Table I and Fig. 4.

As pictured in Fig. 4, for a single set of solutions for (α_1 to α_{14}), corresponding to M' equal to 2.2, a range of solutions for (β_1 to β_{14}) and (γ_1 to y_{14}), corresponding to increasing M from 2.2 to 3, is obtained. For the purpose of verification, the solution for when ($M' = 2.2$) and ($M = 3$) is picked as the operating point of the prototype seven-level CHB inverter. The obtained phase angles in this operating point are listed in Table II. The phase angles in Table II are used to generate the switching functions for the prototype seven-level CHB Converter.

The experimental setup is depicted in Fig. 5. As pictured, the dc-link ports of the CHB converter are connected to 12-V batteries to ensure complete isolation of dc-link voltages. The switching functions for the CHB converter are generated using a TMS320F28335 digital signal processor (DSP) based on the values in Table II. To emulate the fault condition, one of the switches in phase "a" of the inverter is manually short circuited, and to make the phase "a" voltage symmetric around zero, the H-bridge cell containing the faulty switch is bypassed by the DSP. Afterward, the obtained switching angles in Table II are

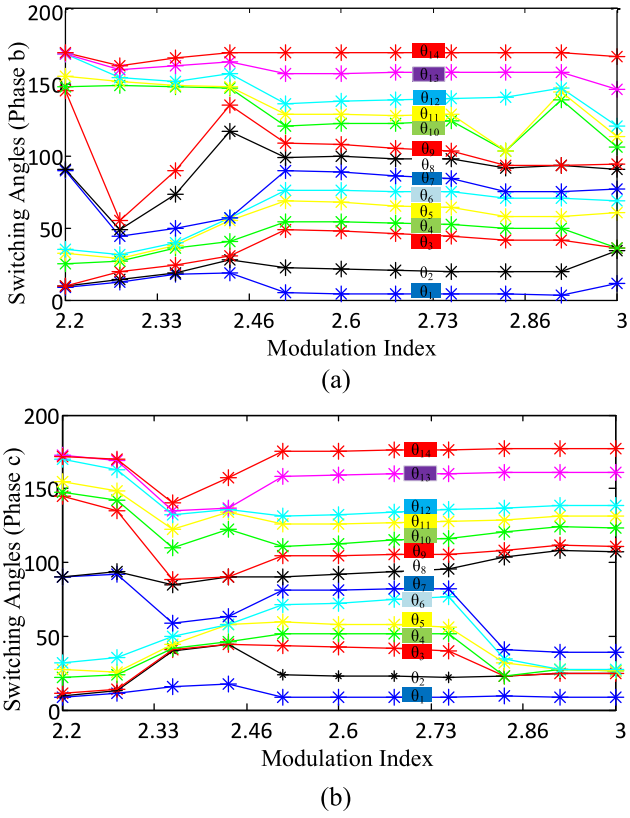

Fig. 4. Obtained switching angles for phase "b" and "c" versus the modulation index (M).

TABLE II
CHOSEN SWITCHING ANGLES (IN DEGREES) FOR PERFORMING THE EXPERIMENTS.

Phase "a"						
α_1	α_2	α_3	α_4	α_5	α_6	α_7
8.47	9.28	9.86	25.25	32.10	35.19	89.76
α_8	α_9	α_{10}	α_{12}	α_{13}	α_{14}	α_{15}
107.62	111.29	123.84	131.11	138.66	160.84	176.69
Phase "b"						
β_1	β_2	β_3	β_4	β_5	β_6	β_7
3.42	19.15	41.79	49.95	57.50	70.77	74.68
β_8	β_9	β_{10}	β_{11}	β_{12}	β_{13}	β_{14}
93.35	93.35	139.01	144.02	146.50	157.62	171.26
Phase "c"						
γ_1	γ_2	γ_3	γ_4	γ_5	γ_6	γ_7
8.69	24.44	24.50	27.31	27.31	27.61	38.94
γ_8	γ_9	γ_{10}	γ_{11}	γ_{12}	γ_{13}	γ_{14}
107.62	111.29	123.84	131.11	138.66	160.84	176.69

used by the DSP to generate the three-phase switching functions according to the proposed fault-tolerant strategy.

Due to the inferior quality of the waveforms in a scope shot, the actual raw data from the oscilloscope are exported to MATLAB for further analysis. The converter's phase voltages, as well as, the harmonic spectrum of all three phase voltages, are plotted in Fig. 6 by MATLAB using the raw data imported from the oscilloscope. As pictured, the faulty phase "a" generates

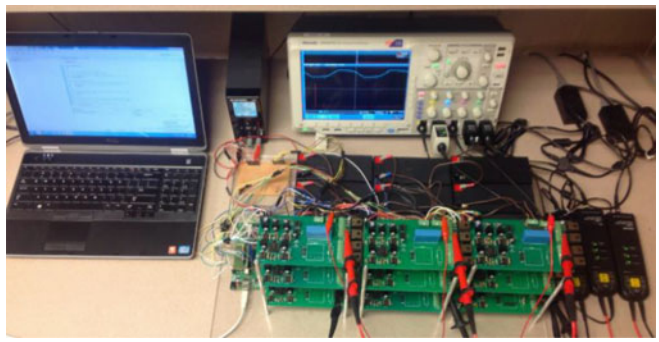

Fig. 5. Prototype three-phase, seven-level CHB converter and TMS320F-28335 controller.

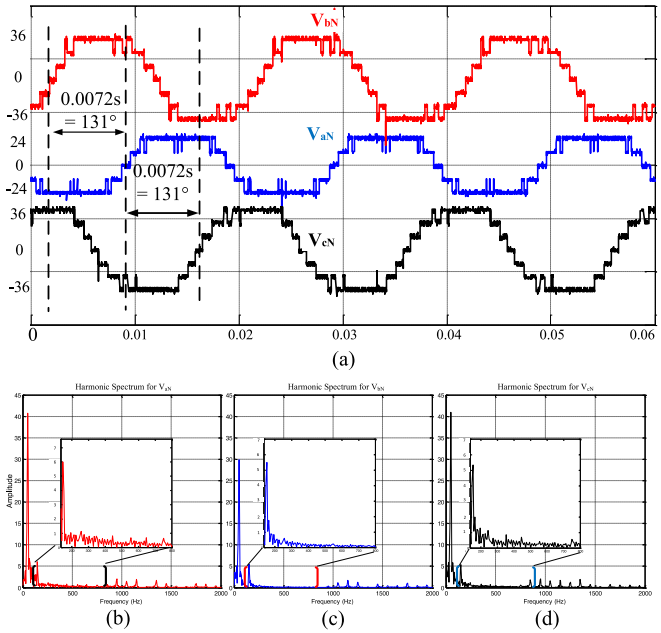

Fig. 6. (a) Experimental CHB converter phase voltages in the event of a single fault at phase "a." (b) Harmonic spectrum for phase "a" voltage. (c) Harmonic spectrum for phase "b" voltage. (d) Harmonic spectrum for phase "c" voltage.

five voltage levels, while the healthy phases generate all seven voltage levels.

According to Fig. 6(a), due to a fault in phase "a", the phase voltages are not balanced, as expected. However, according to the timings marked between the three waveforms, the phase shifts between the waveforms very accurately match the intended values of $\theta_{ab} = \theta_{ca} = 131°$ and $\theta_{ba} = 98°$. This confirms the competence of the proposed modified SHE strategy for manipulation of the angle of the harmonics.

The harmonic spectrum of the phase voltages are plotted in Fig. 6(b)–(d). According to Fig. 6(b)–(d), the amplitude of the fundamental harmonic of "a", "b", and "c" phase voltages are equal to 29.81, 41, and 41 V, respectively. This matches closely with selection of M and M' (2.2 and 3) for solving (13) and proves the capability of the proposed modified SHE strategy for control of the amplitude of the harmonics. The spectrum for the frequency range of 100 to 800 Hz is illustrated in separate zoomed-in windows for better visualization. According to the

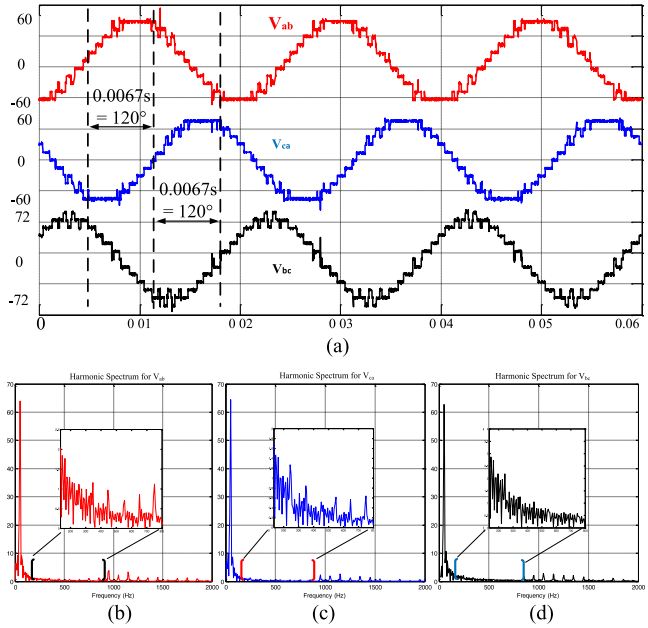

Fig. 7. (a) Experimental CHB converter phase voltages in the event of a single fault at phase "a". (b) Harmonic spectrum of V_{ab}. (c) Harmonic spectrum of V_{ca}. (d) Harmonic spectrum of V_{bc}.

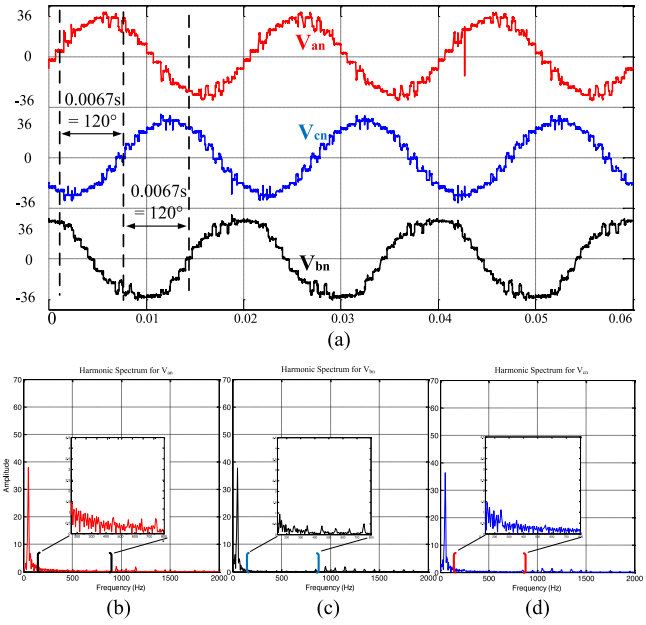

Fig. 8. (a) Experimental CHB converter load voltages in the event of a single fault at phase "a". (b) Harmonic spectrum of V_{an}. (c) Harmonic spectrum of V_{bn}. (d) Harmonic spectrum of V_{cn}.

zoomed-in plots, the amplitudes of the third-order harmonics in three phases are equal as intended. Additionally, the low-order harmonics up to 750 Hz are eliminated as planned. The THD of the phase voltages are calculated from the harmonic spectrum by MATLAB. The resulting values for phases "a", "b", and "c" are 26%, 19%, and 19%, respectively.

To verify generation of balanced line-to-line voltages and the proper placement of the harmonic angles, the line-to-line voltages need to be examined. The line-to-line voltages are traced by the oscilloscope and, similar to before, the raw data are imported to MATLAB to plot Fig. 7. The three-phase line voltages are plotted in Fig. 7(a). According to Fig. 7(a), the amplitudes of the line voltages are all equal (63 V), and the phase shifts between the voltage waveforms are also equal (120°). This confirms the validity of the proposed fault-tolerant strategy for generating balanced line-to-line voltages in the event of a bypassed faulty H-bridge. Similar to before, the harmonic spectrum of the line voltages are plotted in Fig. 7(b)–(d). According to Fig. 7(b)–(d), the third-order harmonics are eliminated naturally in the line voltages. This confirms the proper placement of the third-harmonic angles by the aforementioned innovative reformulation of the SHE problem. The calculated THD for the line voltages is limited to 10.5%.

In order to verify the satisfactory response of the load to the generated voltages, the three-phase load voltages are traced and plotted in Fig. 8. According to this figure, the load voltages are also balanced, and the low-order harmonics are eliminated in the load voltages as well.

VI. Conclusion

In this paper, a fault-tolerant strategy for improving performance of a multilevel inverter under faulty condition was proposed. Using the proposed strategy, the inverter generates balanced line-to-line voltages, even with a faulty switch. Using the conventional fault-tolerant strategies, the maximum achievable line-to-line voltages for a seven-level CHB inverter with a single faulty switch will be reduced by more than 30%; however, the reduction in the voltage when using the proposed method is around only 10%. Additionally, the proposed strategy could eliminate the low-order harmonics of the inverter voltages. The proposed strategy can easily be implemented on various types of multilevel inverters without limitation on the number of voltage levels.

References

[1] M. Malinowski, K. Gopakumar, J. Rodriguez, and M. A. Perez, "A survey on cascaded multilevel inverters," *IEEE Trans. Ind. Electron.*, vol. 57, no. 7, pp. 2197–2206, Aug. 2009.

[2] S. Kouro, M. Malinowski, K. Gopakumar, J. Pou, L. G. Franquelo, B. Wu, J. Rodriguez, M. A. Perez, and J. I. Leon, "Recent advances and industrial applications of multilevel converters," *IEEE Trans. Ind. Electron.*, vol. 57, no. 8, pp. 2553–2580, Jun. 2010.

[3] V. Dargahi, A. K. Sadigh, M. Abarzadeh, M. A. Pahlavani, and A. Shoulaie, "Flying capacitors reduction in an improved double flying capacitor multicell converter controlled by a modified modulation method," *IEEE Trans. Power Electron.*, vol. 27, no. 9, pp. 3875–3887, Mar. 2012.

[4] K. Nguyen-Duy, L. Tian-Hua, C. Der-Fa, and J. Y. Hung, "Improvement of matrix converter drive reliability by online fault detection and a fault-tolerant switching strategy," *IEEE Trans. Ind. Electron.*, vol. 59, no. 1, pp. 244–256, May 2012.

[5] Y. Song and B. Wang, "Survey on reliability of power electronic systems," *IEEE Trans. Power Electron.*, vol. 28, no. 1, pp. 591–604, Apr. 2012.

[6] V. Dargahi, A. K. Sadigh, M. Abarzadeh, S. Eskandari, and K. A. Corzine, "A new family of modular multilevel converter based on modified flying-capacitor multicell converters," *IEEE Trans. Power Electron.*, vol. 30, no. 1, pp. 138–147, Feb. 2014.

[7] L. Hu, M. Ma, A. Chen, X. He, and H. Ma, "Reconfiguration of carrier-based modulation strategy for fault tolerant multilevel inverters," *IEEE Trans. Power Electron.*, vol. 22, no. 5, pp. 2050–2060, Sep. 2007.

[8] M. Aleenejad, H. Iman-Eini, and S. Farhangi, "Modified space vector modulation for fault-tolerant operation of multilevel cascaded H-bridge inverters," *IET Power Electron.*, vol. 6, pp. 742–751, 2013.

[9] M. A. Parker, R. Li, and S. J. Finney, "Distributed control of a fault-tolerant modular multilevel inverter for direct-drive wind turbine grid interfacing," *IEEE Trans. Ind. Electron.*, vol. 60, no. 2, pp. 509–522, Feb. 2012.
[10] L. Jun, A. Q. Huang, L. Zhigang, and S. Bhattacharya, "Analysis and design of active NPC (ANPC) inverters for fault-tolerant operation of high-power electrical drives," *IEEE Trans. Power Electron.*, vol. 27, no. 2, pp. 519–533, Apr. 2011.
[11] B. Mirafzal, "Survey of fault-tolerance techniques for three-phase voltage source inverters," *IEEE Trans. Ind. Electron.*, vol. 61, no. 10, pp. 5192–5202, Jan. 2014.
[12] P. Lezana, J. Pou, T. A. Meynard, J. Rodriguez, S. Ceballos, and F. Richardeau, "Survey on fault operation on multilevel inverters," *IEEE Trans. Ind. Electron.*, vol. 57, no. 7, pp. 2207–2218, Sep. 2009.
[13] N. Davoudzadeh, M. Tafazoli, and M. Sayeh, "On linearity of all optical asynchronous binary delta–sigma modulator," *Opt. Commun.*, vol. 308, pp. 49–53, 2013.
[14] N. Davoudzadeh, M. Tafazoli, and M. Sayeh, "All-optical proteretic (reversed-hysteretic) bi-stable device," *Opt. Commun.*, vol. 331, pp. 306–309, 2014.
[15] L. Shengming and L. Xu, "Strategies of fault tolerant operation for three-level PWM inverters," *IEEE Trans. Power Electron.*, vol. 21, no. 4, pp. 933–940, Jul. 2006.
[16] P. Correa, M. Pacas, and J. Rodriguez, "Modulation strategies for fault-tolerant operation of h-bridge multilevel inverters," in *Proc. IEEE Int. Symp. Ind. Electron.*, 2006, pp. 1589–1594.
[17] S. Ceballos, J. Pou, E. Robles, J. Zaragoza, and J. L. Martin, "Performance evaluation of fault-tolerant neutral-point-clamped converters," *IEEE Trans. Ind. Electron.*, vol. 57, no. 8, pp. 2709–2718, Jul. 2009.
[18] S. Wenchao and A. Q. Huang, "Control strategy for fault-tolerant cascaded multilevel converter based STATCOM," in *Proc. IEEE 22nd Annu. Appl. Power Electron. Conf.*, 2007, pp. 1073–1076.
[19] G. T. Son, H.-J. Lee, T. S. Nam, Y.-H. Chung, U. H. Lee, S.-T. Baek, K. Hur, and J.-W. Park, "Design and control of a modular multilevel HVDC converter with redundant power modules for noninterruptible energy transfer," *IEEE Trans. Power Del.*, vol. 27, no. 3, pp. 1611–1619, Apr. 2012.
[20] P. W. Hammond, "Enhancing the reliability of modular medium-voltage drives," *IEEE Trans. Ind. Electron.*, vol. 49, no. 5, pp. 948–954, Oct. 2002.
[21] K. Shen, B. Xiao, J. Mei, L. M. Tolbert, J. Wang, X. Cai, and Y. Ji, "A modulation reconfiguration based fault-tolerant control scheme for modular multilevel converters," in *Proc. IEEE 28th Annu. Appl. Power Electron. Conf. Expo.*, 2013, pp. 3251–3255.
[22] J. Rodriguez, P. W. Hammond, J. Pontt, R. Musalem, P. Lezana, and M. J. Escobar, "Operation of a medium-voltage drive under faulty conditions," *IEEE Trans. Ind. Electron.*, vol. 52, no. 4, pp. 1080–1085, Aug. 2005.
[23] P. W. Hammond and M. F. Aiello, "Multiphase power supply with series connected power cells with failed cell bypass," U.S. Patent 6 222 284 B1, Apr. 24, 2001.
[24] Z. Yi, W. Xu, X. Bin, and L. Jihong, "Control method for cascaded h-bridge multilevel inverter failures," in *Proc. 6th World Congr. Intell. Control Autom.*, 2006, pp. 8462–8466.
[25] P. Lezana and G. Ortiz, "Extended operation of cascade multicell converters under fault condition," *IEEE Trans. Ind. Electron.*, vol. 56, no. 7, pp. 2697–2703, Apr. 2009.
[26] D. Eaton, J. Rama, and P. Hammond, "Neutral shift [five years of continuous operation with adjustable frequency drives]," *IEEE Ind. Appl. Mag.*, vol. 9, no. 6, pp. 40–49, Nov.–Dec. 2003.
[27] Siemens. The drive of choice for highest demands. [Reliable, precise, and durable]. (2008). [Online]. Available: https://www.swe.siemens.com/spain/web/es/industry/drive_tech/flender/Documents/Folleto%20Robicon%20Perfect%20Harmony.pdf
[28] M. Aleenejad, P. Moamaei, H. Mahmoudi, and R. Ahmadi, "Unbalanced selective harmonic elimination for fault-tolerant operation of three phase multilevel cascaded h-bridge inverters," in *Proc. IEEE Appl. Power Electron. Conf. Expo.*, 2015, pp. 1589–1594.
[29] M. Marchesoni, M. Mazzucchelli, and S. Tenconi, "A non conventional power converter for plasma stabilization," in *Proc. IEEE 19th Annu. Power Electron. Spec. Conf.*, 1988, vol. 1, pp. 122–129.
[30] M. Aleenejad, R. Ahmadi, and P. Moamaei, "Selective harmonic elimination for cascaded multicell multilevel power converters with higher number of h-bridge modules," in *Proc. Power Energy Conf.*, 2014, pp. 1–5.
[31] A. Kavousi, B. Vahidi, R. Salehi, M. Bakhshizadeh, N. Farokhnia, and S. S. Fathi, "Application of the Bee algorithm for selective harmonic elimination strategy in multilevel inverters," *IEEE Trans. Power Electron.*, vol. 27, no. 4, pp. 1689–1696, Aug. 2011.
[32] A. Moeini, H. Iman-Eini, and M. Bakhshizadeh, "Selective harmonic mitigation-pulse-width modulation technique with variable DC-link voltages in single and three-phase cascaded H-bridge inverters," *IET Power Electron.*, vol. 7, pp. 924–932, 2014.
[33] L. Huibo, M. Chengxiong, W. Dan, L. Jiming, and W. Libing, "Fundamental modulation strategy with selective harmonic elimination for multilevel inverters," *IET Power Electron.*, vol. 7, pp. 2173–2181, 2014.
[34] J. R. Wells, B. M. Nee, P. L. Chapman, and P. T. Krein, "Selective harmonic control: A general problem formulation and selected solutions," *IEEE Trans. Power Electron.*, vol. 20, no. 6, pp. 1337–1345, Nov. 2005.
[35] W. Fei, X. Du, and B. Wu, "A generalized half-wave symmetry she-PWM formulation for multilevel voltage inverters," *IEEE Trans. Ind. Electron.*, vol. 57, no. 9, pp. 3030–3038, Dec. 2009.
[36] W. Fei, B. Wu, and Y. Huang, "Half-wave symmetry selective harmonic elimination method for multilevel voltage source inverters," *IET Power Electron.*, vol. 4, pp. 342–351, 2011.
[37] A. Marzoughi and H. Imaneini, "Optimal selective harmonic elimination for cascaded h-bridge-based multilevel rectifiers," *IET Power Electron.*, vol. 7, pp. 350–356, 2014.
[38] N. R. N. Ama, F. O. Martinz, L. Matakas, and F. Kassab, "Phase-locked loop based on selective harmonics elimination for utility applications," *IEEE Trans. Power Electron.*, vol. 28, no. 1, pp. 144–153, Apr. 2012.
[39] J. Napoles, A. J. Watson, J. J. Padilla, J. I. Leon, L. G. Franquelo, P. W. Wheeler, and , M. A. Aguirre, "Selective harmonic mitigation technique for cascaded h-bridge converters with nonequal DC link voltages," *IEEE Trans. Ind. Electron.*, vol. 60, no. 5, pp. 1963–1971, Apr. 2012.
[40] F. Filho, H. Z. Maia, T. H. A. Mateus, B. Ozpineci, L. M. Tolbert, and J. O. P. Pinto, "Adaptive selective harmonic minimization based on ANNs for cascade multilevel inverters with varying DC sources," *IEEE Trans. Ind. Electron.*, vol. 60, no. 5, pp. 1955–1962, Oct. 2012.
[41] A. Marzoughi, H. Imaneini, and A. Moeini, "An optimal selective harmonic mitigation technique for high power converters," *Int. J. Elect. Power Energy Syst.*, vol. 49, pp. 34–39, 2013.
[42] M. S. A. Dahidah, V. G. Agelidis, and M. V. Rao, "On abolishing symmetry requirements in the formulation of a five-level selective harmonic elimination pulse-width modulation technique," *IEEE Trans. Power Electron.*, vol. 21, no. 6, pp. 1833–1837, Nov. 2006.
[43] M. Aleenejad, R. Ahmadi, and P. Moamaei, "A modified selective harmonic elimination method for fault-tolerant operation of multilevel cascaded h-bridge inverters," in *Proc. Power Energy Conf.*, 2014, pp. 1–5.

Mohsen Aleenejad received the B.S. degree in electrical engineering from the AmirKabir University of Technology, Tehran, Iran, in 2010, and the M.S. degree in electrical engineering from the University of Tehran, Tehran, in 2013. He is currently working toward the Ph.D. degree in electrical and computer engineering at Southern Illinois University, Carbondale, IL, USA.

His research interests include power electronics circuits, multilevel converters and their applications in power grid and system, electric-drive vehicles, and solar energy systems.

Hamid Mahmoudi was born in 1989. He received the B.Sc. degree in electrical engineering from the Noshirvani University of Technology, Mazandaran, Iran, in 2011, and the M.Sc. degree in electrical engineering from the Iran University of Science and Technology, Tehran, Iran, in 2014. He is currently working toward the Ph.D. degree in electrical engineering at Southern Illinois University, Carbondale, IL, USA.

His research interests are power electronics, digital control, and motor drives.

Parvin Moamaei received the B.S. degree in electrical engineering from the Nooshirvani University of Technology, Mazandaran, Iran, in 2012. She is currently working toward the Master's degree in electrical and computer engineering at Southern Illinois University, Carbondale, IL, USA.

Her research interests include power electronics, electric drive systems, solar energy, electric drive vehicles, and smart grids.

Reza Ahmadi (M'09) received the B.S. degree in electrical engineering from the Iran University of Science and Technology, Tehran, Iran, in 2009, and the Ph.D. degree in electrical engineering from the Missouri University of Science and Technology, Rolla, MO, USA, in 2013.

He is currently an Assistant Professor of electrical and computer engineering at Southern Illinois University, Carbondale, IL, USA. His research interests include modeling, design and control of power electronic converters, electric-drive vehicles, and solar energy systems.